TECHNISCHE MECHANIK, Band 21, Heft 2, (2001), 91-100
Manuskripteingang: 18. Dezember 2000

Effect of Uniaxial Tensile Loading on the Stiffness of Two-Dimensional Woven SiC/SiC – Modeling and Numerical Simulation

Dedicated to Professor Dr. Dr. h.c. Horst Lippmann on the occasion of his 70th birthday.

H. Ismar, F. Schröter, F. Streicher

The behavior of two-dimensional woven SiC/SiC ceramic matrix composites (CMC) is studied by numerical simulations based on the finite element method (FEM). Starting point of the investigations is a micromechanical model regarding a three-dimensional unit cell. Damage as well as fracture of the single components - fiber bundles and inter yarn matrix - are regarded from a statistical point of view using Weibull distribution. Statements of the behavior of the whole composite are possible by building up a macrostructure. The purpose of the current study is set on the stiffness reduction of the 2Dw composite subjected to tensile loading in one of the fiber directions. Because of the strong anisotropy of the damage a tensor approach is used considering the terms of the elasticity matrix, which are determined for increasing load. Regarding the elasticity matrix the behavior of the composite for any loading situation can be predicted after an arbitrary preloading in one of the fiber direction.

1 Introduction

Ceramic materials have gained improved attention during the last years mainly because of their high strength at elevated temperatures. Their damage behavior however remains a problem. Inhomogenities such as pores or microcracks can lead to brittle fracture even at very low stresses (Ziegler, 1991). Fiber reinforced ceramics - as for example 2D woven SiC/SiC - are a chance to combine the advanced properties of ceramic materials with a damage tolerant behavior. There crack initiation still takes place within the single components - fibers, matrix and fiber-matrix interface - but because of load transfer effects from damaged to undamaged parts the composite shows a damage tolerant behavior. The micromechanical damage effects such as fiber breaking, matrix cracking and fiber-matrix debonding cause a stiffness reduction of the composite. The strength and thus the adaptability of the composite structure change because of the damage evolution. A correlation between the amount of stiffness reduction and the applied loading is of particular interest to estimate the hazard of different loading situations. Within the current paper the reduction of the terms of the elasticity matrix is determined for increasing load in one of the fiber directions. In this way the damage and the anisotropy introduced by damage evaluation can be considered.

2 Modeling the Behavior of 2D Woven SiC/SiC

The modeling of 2D woven structures is strongly affected by the scale on which the composite is regarded (Ladeveze, 1994). Within the current paper the model is constructed on the yarn scale considering two different constituents - fiber bundles and matrix between the fiber bundles, the inter yarn matrix (Guillaumat, 1996; Pluvinage, 1993). The single fibers, the fiber-matrix interface and the matrix within the fiber bundles, the intra yarn matrix, are not considered as single entities during simulation because of computational costs. Both the fiber bundles and the inter yarn matrix are considered to be homogeneous. In Figure 1 a single plane of a 2Dw SiC/SiC structure is shown. 2Dw SiC/SiC composites are usually built up of eight to twelve of such planes. Restricting the observations to a periodical fiber arrangement, the unit cell of Figure 2 can be used to describe the regarded composite structure (Kuo, 1991). There the finite element mesh of the unit cell is shown consisting of 2560 finite matrix and 2560 finite fiber bundle elements. The measures - $a = 0.635$ mm, $b = 0.23$ mm, $c = 0.13$ mm and $d = 0.2896$ mm - given in Figure 2 refer to a fiber volume fraction of 32%. Within the unit cell the volume fraction of the fiber bundles amounts to 54% and the volume fraction of the fibers within the fiber bundles is 60%. By modeling the material behavior on the yarn scale each fiber bundle can be regarded as a unidirectional fiber reinforced composite. The thermal and elastic coefficients of the fiber bundles amount to: $E_1 = 221000$ MPa, $E_2 = 219800$ MPa, $\nu_{12} = 0.214$, $\nu_{23} = 0.193$, $G_{12} = 90400$ MPa,

$\alpha_1 = 3.43 \cdot 10^{-6} \frac{1}{K}$ and $\alpha_2 = 3.38 \cdot 10^{-6} \frac{1}{K}$, where the 1-direction refers to the fiber direction, which is the preferred direction.

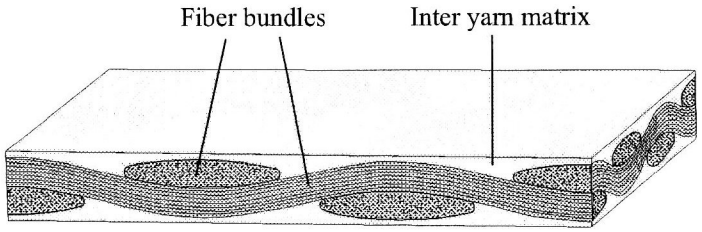

Figure 1. Single Plane of a 2Dw SiC/SiC Composite

The linear elastic behavior of the fiber bundles ends because of crack initiation within the intra yarn matrix. Thereby two cases are to be distinguished depending on the applied loading:

- Cracks develop, which are more or less perpendicularly aligned to the fiber direction. In this case the load which can no longer be borne by the matrix is transferred by the fibers. This behavior is restricted to tensile and compressive stresses in fiber direction.
- Cracks develop parallel to the fiber direction. Thus the load cannot be transferred through the fibers and brittle fracture occurs. This behavior takes place for tensile and compressive loading transverse to the fiber direction as well as for shear loading.

Damage and fracture of the fiber bundles for different loading situations are shown in Figure 3 (Altenbach, 1996; Puck, 1992). Unlike the fiber bundles the isotropic inter yarn matrix - $E = 251000$ MPa, $\nu = 0.16$ and $G = 108000$ MPa and $\alpha = 4 \cdot 10^{-6} \frac{1}{K}$ - only shows brittle fracture because there are no reinforcement components within.

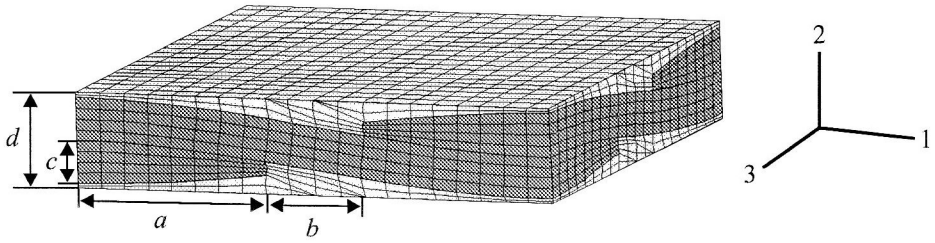

Figure 2. Finite Element Mesh of the Unit Cell Used in Simulations

2.1. Fracture Behavior of the Fiber Bundles and the Inter Yarn Matrix

The flow chart of the crack model used to describe the fracture of the fiber bundles and the matrix is shown in Figure 4. It is considered for each iteration step of the FEM program. Within each iteration the stresses are calculated depending on the actual strain status and the actual elastic coefficients. Afterwards it is checked if this stress state leads to crack initiation. Therefore a fracture criterion is defined for each component. By using a fracture criterion cracking can be regarded considering a complex stress state (Cuntze, 1997; Nahas, 1986). A general fracture criterion is given by Tsai and Wu (Tsai, 1971) as:

$$a_i \sigma_i + a_{ij} \sigma_i \sigma_j = 1 \tag{1}$$

From equation (1) the fracture criteria for the matrix and the fiber bundles can be derived. To describe the fracture of orthotropic materials twelve independent parameters are necessary. Due to the transversely isotropic behavior of the fiber bundles and by neglecting the stress component in fiber direction σ_1 the fracture criterion of the fiber bundles depends only on four parameters:

$$\begin{aligned} &a_2(\sigma_2 + \sigma_3) + a_{22}(\sigma_2^2 + \sigma_3^2 + 2\sigma_4^2) \\ &\quad +2a_{23}(\sigma_2\sigma_3 - \sigma_4^2) + a_{55}(\sigma_5^2 + \sigma_6^2) = 1 \end{aligned} \tag{2}$$

The stress component in fiber direction σ_1 is not considered in equation (2) because σ_1 usually does not lead to crack initiation parallel to the fiber direction. Instead σ_1 is taken into account by determining the damage behavior of the fiber bundles as described below.

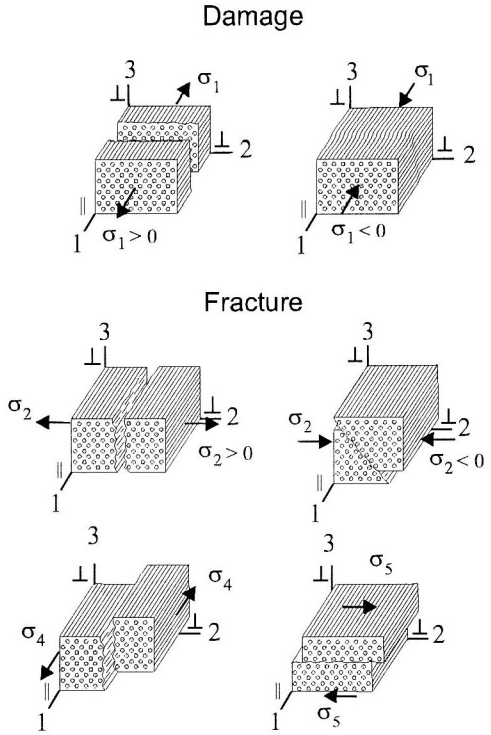

Figure 3. Damage and Fracture of the Fiber Bundles

Three independent parameters are necessary to define the fracture criterion for the isotropic matrix materials as shown in equation (3).

$$a_2(\sigma_1+\sigma_2+\sigma_3)+a_{22}(\sigma_1^2+\sigma_2^2+\sigma_3^2+2\sigma_4^2+2\sigma_5^2+2\sigma_6^2) \\ +2a_{23}(\sigma_1\sigma_2+\sigma_2\sigma_3+\sigma_3\sigma_1-\sigma_4^2-\sigma_5^2-\sigma_6^2)=1 \tag{3}$$

To fix the fracture criteria for the fiber bundles and the matrix as shown in equation (2) and (3) respectively the parameters a_2, a_{22}, a_{23} and a_{55} have to be determined. This can be done by using for example the strength values of uniaxial tensile (R_t), uniaxial compressive (R_c) and shear (R_s) loading. If the fracture criterion is fulfilled for a finite element a crack is introduced into the finite element mesh. This is realized within the used crack model by reducing the elastic coefficients of the regarded element. Thus the topology of the finite element mesh does not have to be varied. To decide which coefficients are to be declined the crack direction is determined by using the energy release rate:

$$G=\frac{dU}{dA} \tag{4}$$

with dA and dU denoting the change in the crack surface and the change in the potential energy. The adaptation of the energy release rate to the requirements of the FEM can be seen in (Ismar, 1995). Within the crack system (e_1^r, e_2^r, e_3^r) - where the direction e_1^r coincides with the crack normal - the elastic coefficients are declined:

$$E_1^r, \nu_{12}^r, \nu_{13}^r, G_{12}^r, G_{13}^r \quad \rightarrow \quad \kappa \cdot E_1^r,\ \kappa \cdot \nu_{12}^r,\ \kappa \cdot \nu_{13}^r,\ \theta \cdot G_{12}^r,\ \theta \cdot G_{13}^r \tag{5}$$

Afterwards the matrix of elasticity is transformed back into the original system (e_1, e_2, e_3) and the stresses are recalculated. To make the fracture model most realistic two further important effects are regarded - the scattering of the strength values as characteristic for ceramics and the post-failure behavior. Several post-failure models can be found in literature (Nahas, 1986). The simplest way is to set both post-failure parameters $\kappa = \theta = 0$ if the fracture criterion is fulfilled. In case of modeling on the microscale considering very small finite elements this model leads to very good results (Ismar, 1999), whereas by

modeling on the yarn scale as done in the current study each finite element is that large, that several cracks can appear within. This multiple cracking observed for 2Dw-SiC/SiC, both within the inter yarn matrix and the fiber bundles (Droillard, 1996; Pluvinage, 1996; Naslain, 1993), is caused by load transfer effects within the composite.

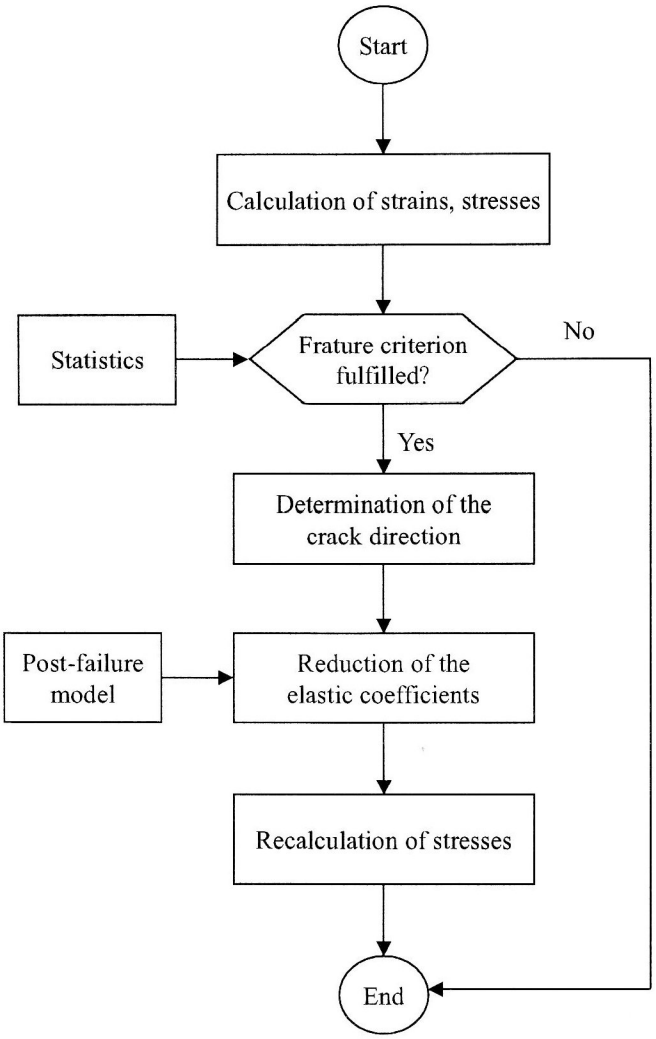

Figure 4. Flow Chart of the Fracture Model Used

Because of this multiple cracking has to be regarded for each finite element where the elastic coefficients depend on the crack number. To interrelate the crack density to the actual stress state the post-failure model of Puck (Puck, 1996) is used. Within this model, there is a distinction between tensile and compressive loading in crack direction. For tensile loading both post-failure parameters are reduced:

$$\kappa = \theta = \eta = \frac{1 - \eta_r}{1 + \zeta(\phi - 1)^{\xi}} + \eta_r \tag{6}$$

where $\xi = 2$ and $\zeta = 4$ are constants to describe the stress reduction and $\eta_r = 0.03$ is the remaining stiffness after crack saturation. For compressive loading only the parameter θ is reduced:

$$\theta = \eta * \cos^2 \varrho + \sin^2 \varrho \qquad \varrho = \arctan|\chi| \qquad \chi = \frac{\sigma_1^r}{\sigma_s^r} \tag{7}$$

The parameter κ remains constant ($\kappa = 1$) because normal stresses in loading direction can still be transferred. Thus the Young's modulus and the Poission's ratios do not have to be reduced. Furthermore shear stresses σ_s^r within the crack plane can be transferred under compressive loading by frictional sliding of the crack surfaces. Because of this θ increases with increasing compressive stress σ_1^r as defined in equation (8), where ϕ is a measure for the crack density within the material. It is involved in the

fracture criterion by multiplying all stress terms with $\frac{1}{\phi}$ and solving the equation for ϕ:

$$\phi = \frac{1}{2}\left[\sum L + \sqrt{(\sum L)^2 + 4\sum Q}\right] \tag{8}$$

$\sum L$ and $\sum Q$ respectively are the sum of first and second order stress terms of the fracture criterion used. They are shown exemplarily for the matrix material in equation (9) and (10).

$$\sum L = a_2(\sigma_1 + \sigma_2 + \sigma_3) \tag{9}$$

$$\begin{aligned}\sum Q = {} & a_{22}(\sigma_1^2 + \sigma_2^2 + \sigma_3^2 + 2\sigma_4^2 + 2\sigma_5^2 + 2\sigma_6^2) \\ & +2a_{23}(\sigma_1\sigma_2 + \sigma_2\sigma_3 + \sigma_3\sigma_1 - \sigma_4^2 - \sigma_5^2 - \sigma_6^2) = 1\end{aligned} \tag{10}$$

To calculate the parameter ϕ the stress terms derived from the actual strain status and the elastic coefficients of the undamaged material have to be used. Thus ϕ always increases with increasing loading corresponding to the crack density. The model introduced by Puck is used to describe the post-failure behavior, because it considers a complex stress state. It is based on the assumption of strength scattering within the material as it is characteristic for ceramic materials. This scattering also has to be considered by determination of crack initiation. Thus within the current paper crack initiation is considered from a statistical point of view involving statistics in the fracture criterion. To do so, the Weibull distribution (Tietz, 1994) is used to describe the scattering of the strength values necessary to define the fracture criterion. The Weibull distribution describes the failure probability of specimen at a given stress σ:

$$P_f(\sigma) = 1 - exp\left[-\left(\frac{\sigma - \sigma^u}{R^0}\right)^M\right] \tag{11}$$

The constant σ^u indicates the stress below which no failure occurs. Because of inhomogenities such as pores or microcracks which are always present in ceramic materials, one cannot exclude failure even in the case of very small stresses, which is why σ^u is assumed to be zero. The Weibull shape parameter M characterizes the dispersion of the failure stress. The higher M the smaller the dispersion and vice versa. Through the parameter R^0 the volume dependence of the failure probability is involved:

$$R^0 = \left(\frac{V^0}{V}\right)^{\frac{1}{M}} \sigma^0 \tag{12}$$

where σ^0 is the stress up to which 63% of the specimens - with a volume V^0 - have failed. V is the volume of the considered specimen. The volume dependence can be explained by the fact that the probability of a critical defect within the regarded volume increases with increasing specimen volume. The Weibull parameters applied to distribute the strength values of the matrix were determined in our experiments. Adapted to the average volume of a matrix element within the finite element mesh of $V = 1.2{\cdot}10^{-13}\mathrm{m}^3$ they conduct to: $R_t^0 = 170$ MPa, $R_c^0 = 2.98 * R_t^0$, $R_{12,s}^0 = 1.35 * R_t^0$ and $M_{ma} = 4$. The strength values of the transversely isotropic fiber bundles were determined by numerical simulations of unidirectional fiber reinforced composites (Ismar, 1999) as: $R_{2,t}^0 = 45$ MPa, $R_{2,c}^0 = 11.0 * R_{2,t}^0$, $R_{23,s}^0 = 1.96 * R_{2,t}^0$, $R_{12,s}^0 = 3.3 * R_{2,t}^0$ and $M_{fb} = 23$, referring to an average volume of $V = 1.4{\cdot}10^{-13}\mathrm{m}^3$. The high value of M_{fb} can be explained by the periodical fiber arrangement considered within the simulations. At the beginning of each simulation the strength values are allocated to the finite elements using Weibull distribution. Thereby only the size of the fracture surface is changed, but not the shape itself. Thus all strength values are given relative to the strength value for tensile loading.

2.2. Damage Behavior of the Fiber Bundles

By loading the fiber bundles in fiber direction the linear elastic behavior ends because of cracking of the intra yarn matrix and fiber matrix debonding. At higher loadings fracture occurs because of multiple fiber breaking. Referring to the coordinate system of Figure 3, the effects mentioned above primarily cause a reduction of Young's modulus in fiber direction E_1, Poission ratios ν_{12} and ν_{13} and the moduli

of shear G_{12} and G_{13}. As the cracks within the intra yarn matrix are more or less perpendicular to the fiber direction the original isotropic behavior of the fiber bundles within the 2-3 plane can be considered to remain after crack initiation: $\nu_{12} = \nu_{13} = \nu_{\parallel\perp}$ and $G_{12} = G_{13} = G_{\parallel\perp}$. Thus, the damage evolution can be described using three damage variables:

$$D_E = 1 - \frac{E_{\parallel}(\varepsilon_{\parallel})}{E_{\parallel}(0)} \qquad D_\nu = 1 - \frac{\nu_{\parallel\perp}(\varepsilon_{\parallel})}{\nu_{\parallel\perp}(0)} \qquad D_G = 1 - \frac{G_{\parallel\perp}(\varepsilon_{\parallel})}{G_{\parallel\perp}(0)} \tag{13}$$

where '0' refers to the initial undamaged material behavior. Within equation (13) the damage is considered in dependence of the strain state $\varepsilon_{\parallel}$ in fiber direction. The evaluation of the damage parameters with increasing load in fiber direction is given in Figure 5.

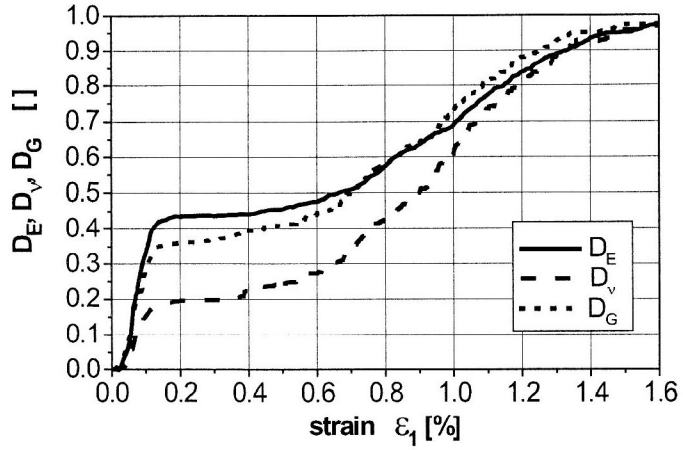

Figure 5. Damage Variables of the Fiber Bundles

They were determined considering numerical simulations to unidirectional fiber reinforced composites (Ismar, 1999). Because of Poisson's ratio effects and the mismatch of thermal coefficients compressive strains in fiber direction appear within the fiber bundles during the simulations even in the case of tensile loading of the unit cell as considered below. To check the hazard of these strains a threshold $\varepsilon_{\parallel} = -0.48\%$ is used, which characterizes the end of linear elastic stress-strain behavior. As the compressive strains detected in the simulations were much smaller than the threshold used, no further modeling of the fiber bundle behavior under these loading conditions was necessary.

3 Simulations

Due to the large bending radii relative to the fiber thickness the stresses resulting from the fiber undulation can be neglected within the simulation. On the other hand the cooling-down process ceramic composites pass through during fabrication is of particular interest. Residual thermal stresses are present within the single components caused by the mismatch of thermal and elastic coefficients. To take these thermal stresses into account, the unit cell is cooled down for the amount of 1000K (Lamon, 1993) before mechanical loading. In a second step the unit cell is loaded by uniaxial tensile load in one of the fiber directions. Different areas can be identified within the diagram of Figure 6. Up to A the unit cells show a more or less linear elastic behavior, which ends because of multiple matrix cracking within the inter and intra yarn matrix (A-B). Another effect occurring between A and B is fiber-matrix debonding. The range between B and C is characterized by crack saturation within the matrix. At this state the load is mainly borne by the fibers orientated in loading direction. The composite shows a more or less constant stiffness within this range. For stresses higher than C there is a further stiffness reduction caused by fiber breaking. Finally there are no longer enough intact fibers to bear the applied load and rupture of the composites occurs at point D. Comparing the stress-strain behavior of unit cells with different randomly distributed strength values a deviation can be clearly identified, especially within the range of matrix cracking (A-B). Between B and D, where the load is mainly borne by the fibers no significant deviation can be identified because of the large number of fibers considered within the unit cell. To get a behavior representative for the whole structure a macrostructure is built up as schematically shown in

Figure 7. Thereby the stress-strain behavior obtained for different unit cells is statistically distributed to the finite elements of the macrostructure. In this way an 'averaging effect' is reached leading to the stress-strain behavior of Figure 8.

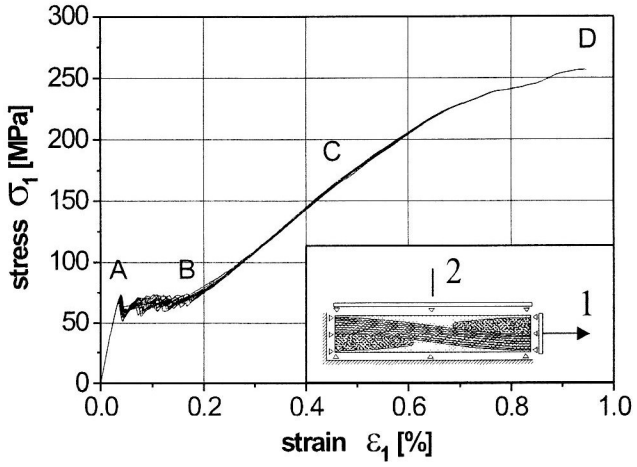

Figure 6. Calculated Stress-Strain Diagrams of the Unit Cell for 20 Simulations

Considering the behavior of at least 20 unit cells the behavior of the macrostructure can be considered to be representative for the whole composite as shown in our former studies (Ismar, 1997). As can be seen in Figure 8 a stiffness reduction of the composite can be identified with increasing load.

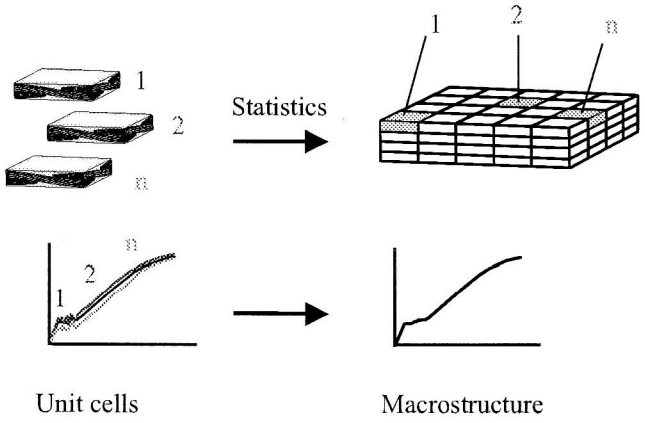

Figure 7. Schematical Building of the Macrostructure

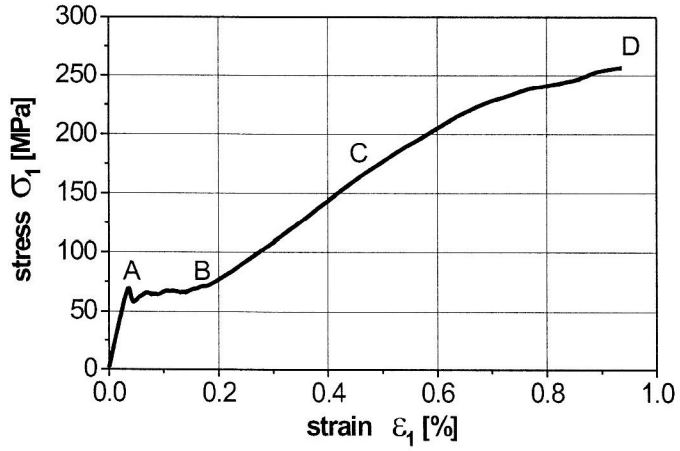

Figure 8. Calculated Stress-Strain Diagram of the Macrostructure

The magnitude of the stiffness degradation depends on the amount of applied loading. The decrease of Young's modulus in 1-direction E_1 of the composite is illustrated in Figure 9. Regarding E_1 the hazard of applied loading can be estimated. Nevertheless, the reduction of Poisson's ratios, shear moduli and Young's moduli E_2 and E_3 cannot be indicated. A more general characterization of damage state involving all elastic coefficient is possible by considering the variation of the matrix of elasticity, as shown in experimental studies (Baste, 1991; Baste, 1992; Baste, 1996).

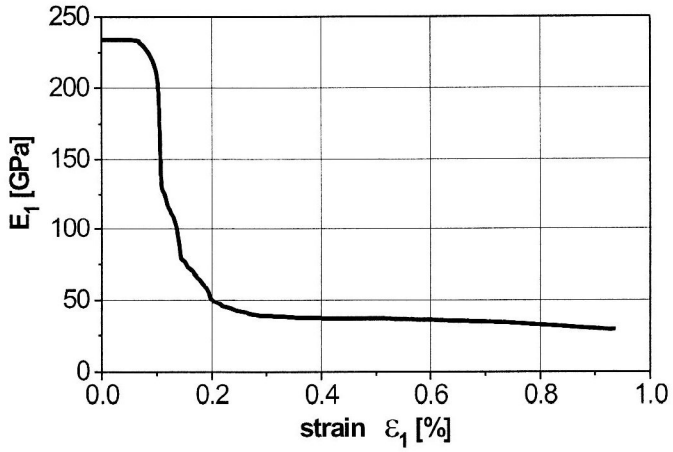

Figure 9. Evaluation of Young's Modulus E_1

Such a general description of damage is desirable for example in the case of changing loads. For an orthotropic material behavior as considered for the 2Dw composite the matrix of elasticity can be written as follows:

$$\begin{bmatrix} C_{11} & C_{12} & C_{13} & 0 & 0 & 0 \\ C_{12} & C_{22} & C_{23} & 0 & 0 & 0 \\ C_{13} & C_{23} & C_{33} & 0 & 0 & 0 \\ 0 & 0 & 0 & C_{44} & 0 & 0 \\ 0 & 0 & 0 & 0 & C_{55} & 0 \\ 0 & 0 & 0 & 0 & 0 & C_{66} \end{bmatrix} \tag{14}$$

Regarding the elasticity matrix as defined in equation (14) the load bearing capacity for any loading direction can be determined. Thus the hazard of different loading situations can be checked. The evaluation of the components of the matrix of elasticity for increasing straining in one of the loading directions is shown in Figure 10. As a result of the symmetry of the woven structure the initial stiffness along the 1-direction corresponds with the one in 3-direction as well as the shear stiffnesses C_{44} and C_{66}. A first derivation may appear during the cooling-down process because of anisotropic crack initiation due to the statistical distribution of the strength values. Within the regarded simulations cracking could only be identified for several finite elements with very low strength values during cooling-down process. Regarding for example the stiffness in loading direction C_{11} in Figure 10 the areas explained in Figure 8 - 0-A, A-B, B-C, C-D - can also be identified. The initial linear elastic behavior ends because of multiple matrix cracking. The small size of the strain interval of matrix cracking can be explained by the low strength of the considered SiC matrix. An area characterized by crack saturation and no further decrease of stiffness follows. The reduction of elastic coefficients continues after the start of fiber breaking. Finally rupture of the composite takes place caused by extensive fiber breaking at about $\epsilon_1 = 0.94\%$. Comparing the different terms of stiffness the anisotropy of the damage can be verified. An important loss of stiffness along the loading axis (axis 1) can be notified. It is also worth noting that the damage evolution strongly affects the shear moduli of the planes containing the loading direction C_{44} and C_{66}. As mentioned above the stiffness loss is caused by the evaluation of microcracks mainly within the matrix. The strong anisotropy of the damage evolution can be explained by the predominant orientation of these microcracks. Cracks preferentially grow in the plane transverse to the loading direction destroying the symmetry of the composite structure. The preferred orientation of the microcracks results in a strong reduction of the coefficients C_{11}, C_{12}, C_{13}, C_{44} and C_{66}. On the other hand the reduction of C_{22}, C_{23}, C_{33} and C_{55} is much less. The reduction of stiffness C_{22} along axis 2 as well as of the shear stiffness C_{55} is even negligible. Because of the damage induced anisotropy the directions 1 and 3 are no longer

symmetrically equivalent under load: $C_{11} \neq C_{33}$, $C_{12} \neq C_{13}$ and $C_{44} \neq C_{66}$.

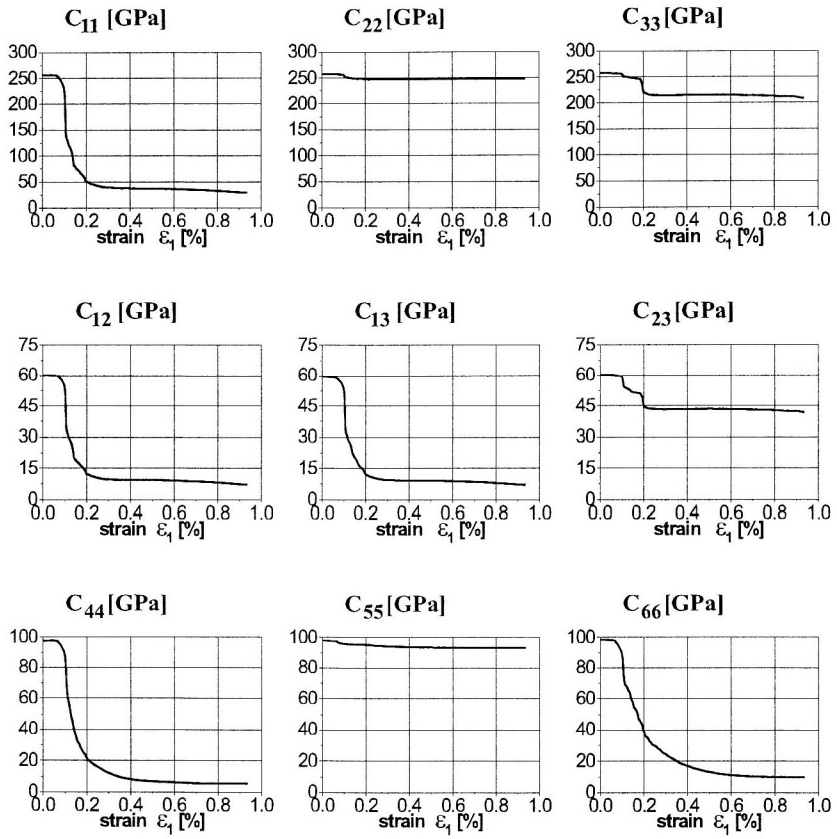

Figure 10. Evaluation of the Terms of Elasticity Matrix for Increasing Load

4 Summery

2Dw SiC/SiC composites are a chance to use the good properties of ceramics without a brittle damage behavior. Though the single components still show brittle fracture, the composite possesses a damage tolerant behavior. The model used to describe the composite behavior is based on a micromechanical approach. Thus crack initiation within the different components as well as residual thermal stresses resulting from a cooling-down process of the composite during fabrication could be taken into account. By using a material model adopted to the behavior of ceramic fiber composites, damage and fracture of the single components could be regarded from a statistical point of view. Besides the characterization of the unit cell a description of the composite behavior was possible by building up a macrostructure.

The main focus of the study was the examination of the damage evaluation of the composite. The micromechanical damage events within the single components could be identified on the macroscale as a reduction of stiffness. The amount of stiffness reduction can be used to characterize the damage state of the composite. A tensor approach was necessary to describe the anisotropy of damage generated by the preferred direction of microcracking. Considering the matrix of elasticity the degree of anisotropy could be studied. The knowledge of the anisotropic reduction of stiffness is especially important in the case of changing loads. Considering the matrix of elasticity the load bearing capacity of the composite for any loading situation can be calculated after an arbitrary preloading in one of the fiber directions.

Literature

1. Altenbach, H.; Altenbach, J.; Rikards, R.: Einführung in die Mechanik der Laminat- und Sandwichtragwerke. Deutscher Verlag für Grundstoffindustrie, Stuttgart, (1996).
2. Baste, S.; Audoin, B.: On internal variables in anisotropic damage. European Journal of Mechanics A / Solids 10, (1991), 587-606.

3. Baste, S.; El Guerjouma, R.; Audoin, B.: Effect of microcracking on the macroscopic behaviour of ceramic matrix composites: Ultrasonic evaluation of anisotropic damage. Mechanics of Materials 14, (1992), 15-31.

4. Baste, S.; El Bouazzaoui, R.: Cracking orientation and induced anisotropy of a ceramic matrix composite under off-axis loading. Journal of Materials Science 31, (1996), 1575-1584.

5. Cuntze, R; Deska, R.; Szelinski, B.; Jeltsch-Fricker, R.; Meckbach, S.; Huybrechts, D.; Kopp, J.; Kroll, L.; Gollwitzer, S. u. Rackwitz, R.: Neue Bruchkriterien und Festigkeitsnachweise für unidirektionalen Faserkunststoffverbund unter mehrachsiger Beanspruchung - Modellbildung und Experimente. VDI Fortschritt-Berichte Reihe 5 Nr. 506, (1997).

6. Droillard, C.; Lamon, J.: Fracture toughness of 2-D woven SiC/SiC CVI-composites with multi-layered interphases. Journal of The American Ceramic Society 79, (1996), 849-858.

7. Guillaumat, L.; Lamon, J.: Probabilistic-statistical simulation of the non-linear mechanical behavior of a woven SiC/SiC composite. Composite Science and Technology 56, (1996), 803-808.

8. Ismar, H.; Reinert, U.: Modelling of the micromechanical behaviour of unidirectional fibre-reinforced ceramics by the example of SiC/SiC, Archive of Applied Mechanics 66, (1995), 34-44.

9. Ismar, H.; Streicher, F.: Modelling and simulation of the mechanical behavior of ceramic matrix composites as shown by the example of SiC/SiC. Computational Materials Science 16, (1999), 17-24.

10. Ismar, H.; Reinert, U.: Modelling and simulation of the macromechanical nonlinear behaviour of fibre-reinforced ceramics on the basis of a micromechanical-statistical material description. Acta Mechanica 120, (1997), 47-60.

11. Kuo, W.-S.; Chou, T. W.: Nonlinear thermomechanical behavior of woven ceramic composites. Proceedings of The American Society for Composites. Sixth Technical Conference, Albany, (1991), 611-620.

12. Ladeveze, P.; Gasser,A. ; Allix, O.: Damage mechanisms modeling for ceramic composites. Journal of Engineering Materials and Technology 116, (1994), 331-337.

13. Lamon, J.; Lissart, N.; Rechiniac, C.; Roach, D. H.; Jouin, J. M.: Micromechanical and statistical approach to the behavior of CMC's. Ceramic Engineering and Science Proceedings 14, (1993), 1115-1124.

14. Nahas, M. N.: Survey of failure and post-failure theories of laminated fiber-reinforced composites. Journal of Composites Technology and Research 8, (1986), 138-153.

15. Naslain, R.: Fibre-matrix interphases and interfaces in ceramic matrix composites processed by CVI. Composite Interfaces 1, (1993), 253-286.

16. Pluvinage, P.; Quenisset, J. M.: Numerical simulation of the tensile behavior of 2D-SiC/SiC cross-ply laminates. Journal of Composite Materials 27, (1993), 152-174.

17. Pluvinage, P; Parvizi-Majidi, A.; Chou, T. W.: Damage characterization of two-dimensional woven and three-dimensional braided SiC-SiC composites. Journal of Materials Science 31, (1996), 232-241.

18. Puck, A.: Praxisgerechte Bruchkriterien für hochbeanspruchte Faser-Kunststoff-Verbunde. Kunststoffe 82, (1992), 149-155.

19. Puck, A.: Festigkeitsanalyse von Faser-Matrix-Laminaten: Modelle für die Praxis. Carl Hanser Verlag München, (1996).

20. Tietz, H.-D.: Technische Keramik: Aufbau, Eigenschaften, Herstellung, Bearbeitung, Prüfung. VDI-Verlag, Düsseldorf, (1994).

21. Tsai, W.; Wu, E. M.: A general theory of strength for anisotropic materials, Journal of Composite Materials 5, (1971), 58-80.

22. Ziegler, G.: Entwicklungstendenzen der Hochleistungskeramik. Ceramic Forum International / Bericht der DKG 68, (1991), 72-79.

Address: Prof. Dr.-Ing. H. Ismar, Dr.-Ing. F. Schröter, Dr.-Ing. F. Streicher, Lehrstuhl für Technische Mechanik, Universität des Saarlandes, Postfach 15 11 50, D-66041 Saarbrücken.
$e-mail$: h.ismar@mx.uni-saarland.de